The Logic of the Auger Hybrid Design

Paul Sommers
High Energy Astrophysics Institute
Physics Department
University of Utah
Salt Lake City, Utah 84112

January 7, 1997

Abstract

The Pierre Auger Project is an international collaboration to study the highest energy cosmic rays. With installations in the northern and southern hemispheres, the Auger Observatory will achieve uniform exposure to the entire celestial sphere, with the enormous collecting power needed for definitive studies of the extremely low cosmic ray intensity near the Greisen-Zatsepin-Kuzmin suppression. This note reviews the reasoning that has led to the hybrid design of a vast surface array of particle detectors along with air fluorescence detectors that observe the atmosphere above the array.

1 Anisotropy studies

It has long been surmised that the highest energy cosmic rays are an extragalactic population whose sources are independent of the galactic cosmic ray population that is observed with balloons, satellites, and small air shower detectors. This inference is based partly on the fact that no obvious anisotropy has been observed, even at the highest energies where the galactic magnetic field should only slightly deflect the particles. The transition from galactic to extragalactic cosmic rays is presumed to occur at the "ankle" of the spectrum, just below 10 EeV. It is the only spectral feature that is suggestive of a transition from one population to another. To study the extragalactic population above the ankle requires an observatory of enormous collecting power, since the integral intensity above 10 EeV is only $0.5/(\mathrm{km}^2 \cdot \mathrm{sr} \cdot \mathrm{yr})$. In 1992, Jim Cronin [1] suggested an international effort to construct a giant detector for this purpose, and that suggestion has been developed through a series of workshops into the specific Auger Observatory design proposal that is now under review.

The expression "collecting power" will here refer to the product of aperture and duty factor (which is the fraction of time that the detector can operate). This product is the same as the exposure rate and can be measured in units of $\mathrm{km}^2 \cdot \mathrm{sr} \cdot \mathrm{yr/yr}$. Multiplying the exposure rate (collecting power) by the cosmic ray intensity gives the number of showers collected per year. For an observatory with a duty factor of 1, the aperture and exposure rate are identical. The Auger surface array has an exposure rate or aperture of 14,000 $\text{km}^2\cdot\text{sr}\cdot\text{yr}/\text{yr}$ for showers above 10 EeV. An all-fluorescence observatory with a duty factor of 0.1 would need an aperture of 140,000 $\text{km}^2\cdot\text{sr}$ to achieve the same exposure rate.

The most direct information about the extragalactic cosmic ray sources above 10 EeV should come from anisotropy studies. Fly's Eye data analysis [2] suggests that those particles are not highly charged heavy nuclei. They are therefore magnetically rigid enough that only modest magnetic deflection can be attributed to their passage through the Galaxy en route to the Earth or to their passage through intergalactic magnetic fields over distances up to the order of 100 Mpc. With adequate statistics, therefore, discrete sources closer than 100 Mpc can be expected to show up as celestial regions of enhanced intensity. This is especially true above 40 or 50 EeV, since the Greisen-Zatsepin-Kuzmin (GZK) suppression then restricts pathlengths to distances less than about 100 Mpc, so more highly deflected arrival directions are automatically removed from the picture. Discrete sources should be detectable. If none are observed, that would imply that there are very many contributing sources closer than 100 Mpc, perhaps transient phenomena like topological defect annihilations or gamma ray bursts instead of persistent cosmic ray emitters.

Figure 1 shows some hypothetical 3-year data sets for arrival directions of showers above 40 EeV. In each case it is assumed that there are a number of discrete persistent sources. The sources are assumed to have approximately equal intensity, and arrival directions from each source have been smeared by sampling from a 2-dimensional Gaussian with $\sigma = 10°$. The actual amount of magnetic dispersion depends on the source distance, intervening magnetic field strengths and coherence lengths, and also the range of magnetic rigidities for the observed particles. The hypothesis of 10° smearing is a crude guess, which might be overestimating the dispersion. Recent analysis of AGASA data [3] suggests that there might be much tighter clustering. Even for 120 equally contributing sources with 10-degree smearing, a clumpy deviation from isotropy is evident in figure 1.

The AGASA event clusters above 40 Eev [3] are suggestive of persistent discrete sources. Of the 36 events, there are 3 pairs of events whose directions cannot be resolved by the detector. If at least one of those pairs is genuinely a source contributing 2/36 of the total cosmic rays, then the Auger Observatory should rapidly acquire enough statistics to study properties of the source(s) and possibly the intervening magnetic fields. Since AGASA does not get the exposure of the Auger southern observatory, the assumption should be that 1/36 of the Auger events above 40 EeV would be from a single discrete source. On that basis, the Auger Observatory would expect to record 11 showers per year from such a source.

In almost any scenario of cosmic ray production, the sources should be distributed like the large scale mass distribution in the region of the universe out to 100 Mpc. The visible matter, at least, is not uniformly distributed but is concentrated preferentially toward the supergalactic plane. Above about 50 EeV, therefore, one expects a prominent (l=2,m=0) spherical harmonic component when analyzed in supergalactic coordinates. There have been some tantalizing suggestions of cosmic ray anisotropy relative to the supergalactic plane in analyses of Haverah Park and AGASA data. The H.P. data suggest a broad equatorial excess [4] that can be described as a supergalactic polar deficit, whereas the

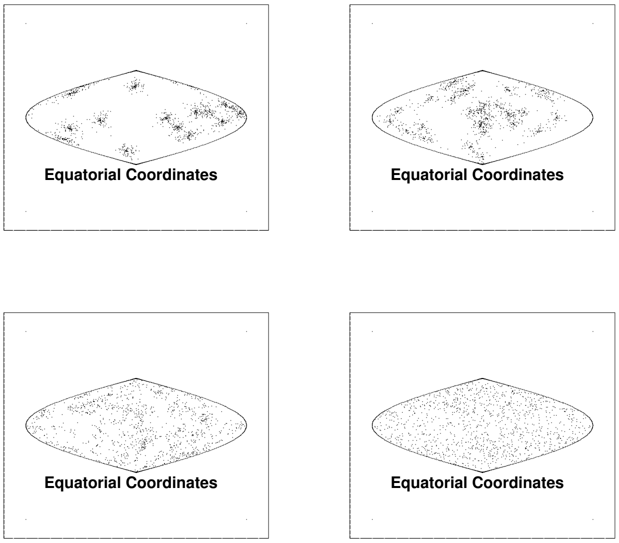

Figure 1: Simulations of the Auger sky above 40 EeV after 3 years. The expected number of showers is 1165. The bottom right is a simulation of isotropy. The other 3 figures simulate a number of equally strong discrete sources, and each source is smeared with a 10-degree Gaussian. Top left: 15 sources. Top right: 30 sources. Bottom left: 120 sources.

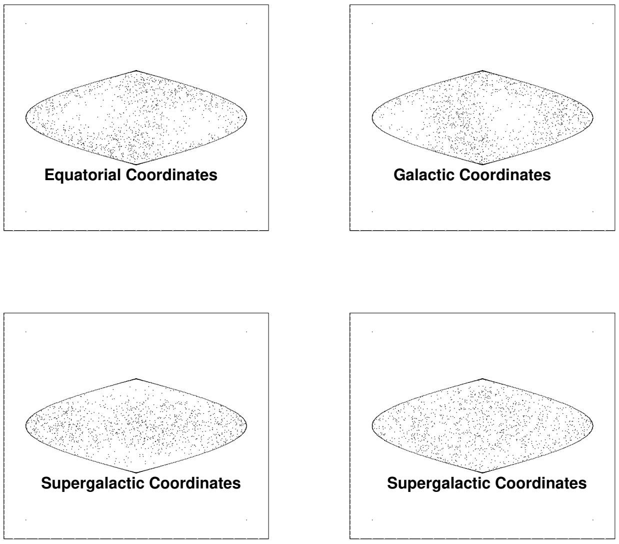

Figure 2: Simulations of the Auger sky above 40 EeV after 3 years, assuming the cosmic ray intensity depends on supergalactic latitude like $\cos^2 b_{sg}$. The observed celestial distribution is shown in 3 different coordinate systems. The lower right figure is a simulation of isotropy for comparison.

AGASA data suggest a narrow excess at the supergalactic equator with no polar deficit [3]. In each case, the number of events is too small for confidence in the suggested anisotropy.

Figure 2 shows the Auger sky for cosmic rays above 40 EeV after 3 years, assuming that the broad equatorial excess suggested by the Haverah Park data is real and there are no discrete sources observed. In those simulations, the Auger installations were assumed to be at +40 and -40 degrees latitude, each with uniform acceptance out to 45 degrees zenith angle. The cosmic ray intensity is assumed to have a dependence on supergalactic latitude given by $\cos^2 b_{sg}$, where b_{sg} is supergalactic latitude. The 1165 events are adequate to produce a 16-sigma effect.

The primary objective of the Auger Project has always been to measure a large number of extragalactic cosmic ray arrival directions with uniform exposure to the entire celestial sphere. With a mid-latitude installation in both the northern and southern hemispheres, the Observatory will have exposure to all arrival directions. Operating continuously, the surface arrays will get uniform exposure in right ascension. There will be a slight non-uniformity in declination. Since that non-uniformity is precisely known from the detector's acceptance dependence on zenith angle, it can be corrected by, for example, discarding each event with a probability determined by the overexposure of its declination. Since the exposure is almost uniform to begin with, this procedure discards few events. Achieving truly uniform exposure is necessary for the most sensitive search for dipole and quadrupole moments as well as analyses with spherical harmonics. It also simplifies the search for discrete sources. For the sake of uniform exposure, it is vital to have matching installations in the northern and southern hemispheres, to build them simultaneously, and operate them continuously.

The Auger Project seeks the greatest possible collecting power consistent with the fiscal realities of our time. It is essential to minimize the cost per shower above 10 EeV. A sparse array of water Cernekov detectors has emerged as the obvious cost-effective way to detect such showers.

Anisotropy analyses represent the best hope for identifying and studying the sources of the highest energy cosmic rays. It is important to have exposure to the entire sky, and it is essential to have the largest affordable collecting power. Because of unavoidable magnetic deflections, high precision in measured arrival directions may be unimportant, and precise energy measurements are not essential for anisotropy analyses. The sparse surface array is completely satisfactory while being the most economical detection method.

2 Energy spectrum

Independent of any anisotropy that may or may not be observed, the energy spectrum of cosmic rays can provide important information about their sources and their propagation [5]. The details of the energy spectrum may depend on properties of the population of sources (e.g. the distribution of maximum rigidity of produced particles and magnetic confinement at the sources). It also is affected by the GZK suppression and therefore is sensitive to the distribution of source distances. The spectrum predicted for the topological defect annihilation scenario is markedly different from any prediction based on accelerative mechanisms. The topological defect scenario predicts an "energy gap" due to the GZK effects, and the gap's structure can depend on the spatial distribution and past evolution of the topological defects.

Accurate and verifiable measurements of air shower energies are essential for extracting specific information about the nature of cosmic ray sources from detailed structure in the energy spectrum.

If it turns out that there are observable discrete sources, then much can be learned by studying the showers coming from those particular directions. The source's energy spectrum is of special interest for understanding the astrophysical processes which account for the high energy cosmic rays. Also, by correlating energies with magnetic deflections from a known source, it is possible to learn much about the intervening magnetic fields, both galactic and extragalactic. Accurate energy measurements are crucial for this.

A major function of the Auger fluorescence detectors is to provide accurate energy measurements without reference to any specific hadronic interaction model. A reliable measurement of a shower's longitudinal profile gives an unambiguous measurement of the energy in its electromagnetic cascade. This is a firm lower limit for the cosmic ray's energy and it leads to the best estimate for the actual energy.

Hadronic interaction models extrapolated from energies probed with laboratory colliders predict that approximately 90% of of the primary's energy is dissipated by the electromagnetic cascade resulting from neutral pion decays. The remaining energy is in the form of muons and neutrinos, primarily from charged pion decays. There is some dependence on the primary particle's mass. A proton shower typically dissipates about 95% of its energy in the electromagnetic cascade whereas the fraction for an average iron shower is closer to 85%. By assuming that the electromagnetic shower energy represents 90% of the total, the systematic error should not be greater than 5%, regardless of what the mass distribution may be. The error on any individual shower energy can be greater than this because of fluctuations in the fraction of energy taken by muons and neutrinos, but if the shower energy is assumed to be 1/0.9 times the electromagnetic energy, then the systematic error should not exceed 5%.

Those hadronic models are not unquestionably correct, since they have not been tested experimentally. It is possible to devise consistent models in which a large amount of the primary energy is frequently given to prompt muons or other particles that do not contribute to the electromagnetic cascade. In that case, shower energies derived from measurements of the electromagnetic cascade could be systematically too low. There is no evidence supporting any such hypothesis, however. It should also be noted that such a model would imply that the mysterious super-GZK particles might be even farther beyond the expected spectral cutoff than has been claimed.

The surface array also has good capability for measuring shower energies, and the two components of the hybrid detector serve as cross checks on each other. The surface array is limited to measuring the cascade at just one atmospheric depth, so the calorimetric method of the fluorescence detector is not available, and an error in the hadronic model could cause systematic error in electromagnetic shower energies as well as total shower energies. As discussed in the next section, the hybrid data set should provide an algorithm for eliminating that source of error, so the entire data set from the surface array can also be used for a high-statistics energy spectrum determination.

The surface array will also play an important role in the hybrid spectrum determination by giving an easy-to-compute aperture. The energy of each shower detected by the surface array while the fluorescence detector is operating should have a high quality fluorescence-assisted energy determination. To convert the energy distribution to a spectrum, one also needs to know the aperture accurately as a function of energy. Atmospheric variation can make that difficult to calculate for a fluorescence detector alone. With a hybrid detector, the aperture can be computed simply with the surface detector acceptance and fluorescence detector runtime.

The surface array and fluorescence detector work symbiotically in measuring shower energies in hybrid mode. Each gives an estimate for the shower size at the surface, and the two estimates serve as cross checks when both are well measured. For some showers measured at long range by the fluorescence detector, the surface array's estimate of shower size provides a valuable way to check the atmospheric attenuation. If the attenuation uncertainty is large for distant events on some nights, the surface array's size determination offers a way to normalize the longitudinal profile.

The idea of an infilled array was considered in order to gain sensitivity also to cosmic rays at lower energies. This is unnecessary, however, with the hybrid design. The fluorescence detector in combination with the sparse array provides high resolution measurements down to about 1 EeV. Although the aperture is smaller than at 10 EeV, there will be ample statistics due to the higher cosmic ray intensity. Detailed simulations have confirmed that the detector will make quality shower measurements at the lower threshold in hybrid mode [6]

It was recognized [7] prior to the first Paris workshop in 1992 that measuring a shower with a single fluorescence detector along with the ground array would provide good geometrical reconstruction, so stereoscopic fluorescence measurements are not necessary. The hybrid design was tentatively adopted at that Paris meeting and developed further at subsequent workshops and in the literature [8] [9]. Some experimental tests of the hybrid technique have been performed using CASA/MIA/HiRes data [10].

3 Primary masses

The surface array is the cost-effective way to get the high statistics and uniform exposure needed for a sensitive anisotropy analysis, and the fluorescence detector provides reliable energy measurements for the energy spectrum. When it comes to determining the cosmic ray mass composition, however, it is the combination of the two detector components that is crucial. The hybrid data set will have high sensitivity to the primary masses.

Knowing the particle types is essential for an understanding of the high energy cosmic ray sources. If there are nuclei other than protons, for example, then the top-down scenarios involving massive particle decays can be excluded. The presence of heavy nuclei would also constrain the photon environment of any astrophysical accelerator since high energy nuclei would photodisintegrate at the source if photon densities are high. Since energetic nuclei can also photodisintegrate while in transit as a result of collisions with cosmic microwave and infrared photons, the distribution of particle masses is a useful handle on the distribution of pathlengths from the sources. The study of the high energy composition should also include a search for photon primary particles. A strong component of primary photons would suggest top-down production processes.

If discrete sources are identified, then it will be important to study the composition of particles coming from each of them. The particle masses will say much about the astrophysical conditions and processes at the source. Since the arrival directions will also be used to probe intervening magnetic fields, it is important to know the rigidities of the detected cosmic rays. Measuring the energy is not enough. The charges of the particles must also be estimated. Since a nuclear charge is approximately half the nucleon number, it suffices to determine the masses of cosmic ray particles.

Given an accurate energy estimate, the muon content of a shower is the most powerful indicator of the primary mass. Heavier nuclei produce showers with more muons. An iron shower produces, on average, 80% more muons than a proton shower of equal total energy. There is very little hadronic model dependence in this fact. It is largely due to the heavy nucleus breaking up to form subshowers of its individual nucleons. Relative muon numbers are therefore a model-independent effective handle on the primary mass.

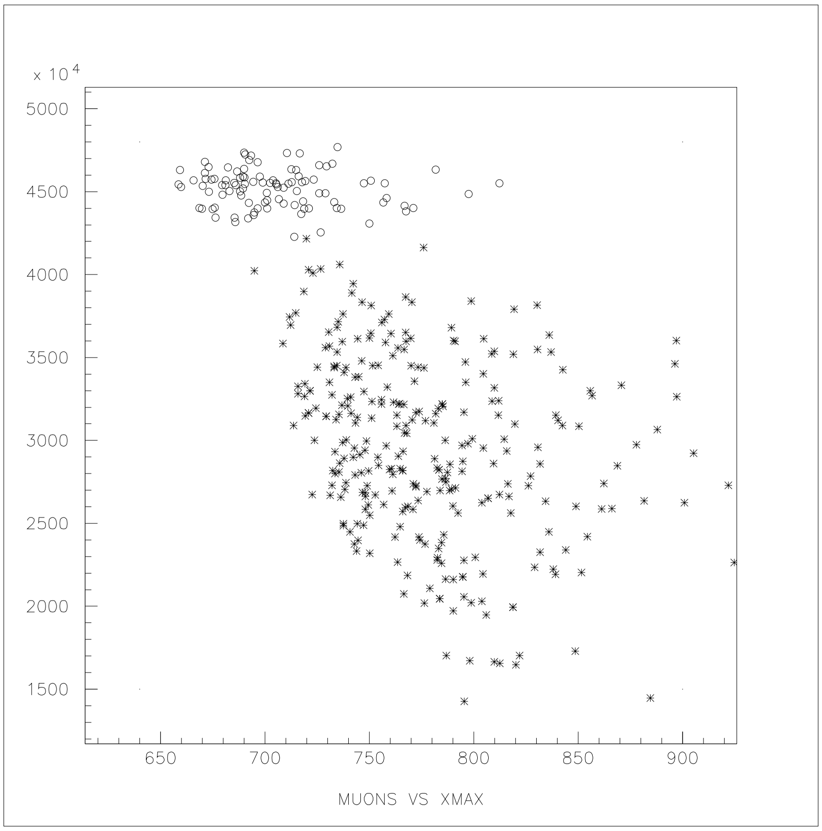

Figure 3: The scatter plot of muon number versus atmospheric depth of maximum. Open circles represent iron showers. The asterisks are proton showers. No experimental resolution has been simulated. The two particle types can be more cleanly separated on the basis of muon number than by depth of maximum.

Figure 3 shows a scatter plot of muon number vs. depth of maximum (X_{max}) for showers of fixed energy. Iron and proton showers are indicated by different symbols. It can be seen that the muon number is a better separator of the two components than is X_{max}.

In practice, experimental measurement fluctuations will limit the utility of muon measurements for primary mass determination. Instead of measuring the total muon number, the surface array will only sample the density with 5 or more $10m^2$ water tanks, and muons can be individually counted only at large distances from the core. Even if muon identification is perfect, Poisson fluctuations in the numbers will introduce an important resolution limitation. (The muon density 1 km from the core is on the order of $1/m^2$ for 10 EeV showers. With 5 detectors triggering, the expected number is on the order of 50. Poisson fluctuations should be on the order of 20% or less at the threshold energy of 10 EeV. The Poisson fluctuations are smaller at higher energies.) When coupled with experimental uncertainty in the shower energy, these resolution limitations may blur even the extreme mass components of iron and protons. Figure 4 shows what happens to the

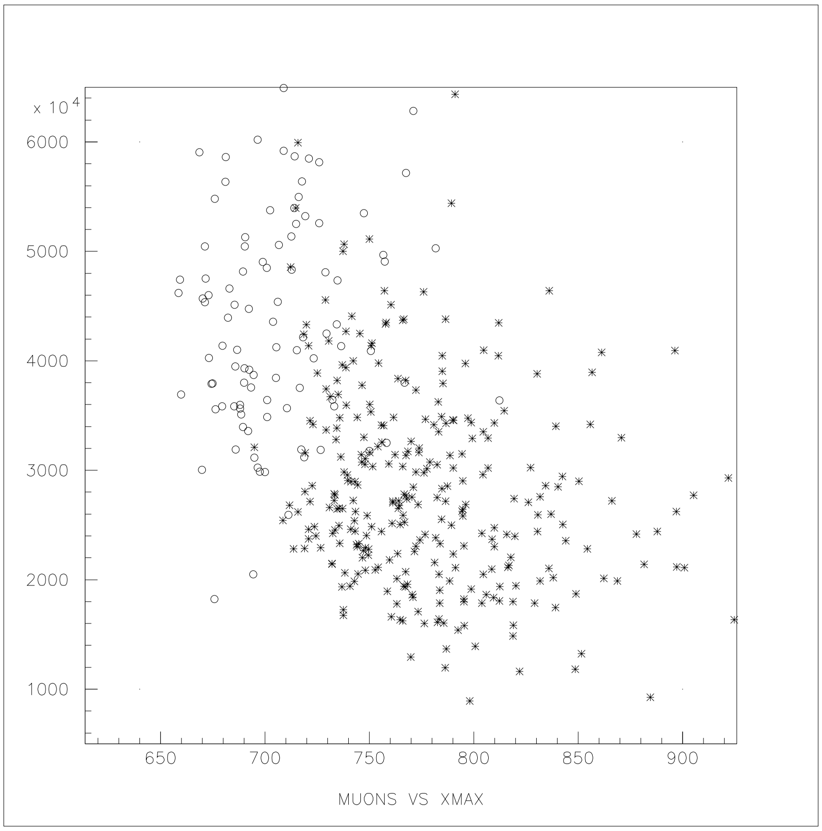

Figure 4: Similar to figure 3, but now a 20% resolution in muon number has been included in the simulation.

scatter plot of figure 3 when the muon number is offset by an amount drawn from a Gaussian with σ=20%. The iron and proton distributions then overlap both in muon content and X_{max}. It is important to note, however, that the smeared distributions can be better separated by a diagonal line in that 2-dimensional scatter plot than they can be separated on the basis of either muons or X_{max} alone. In other words, the two handles, muons and X_{max}, provide a far better mass indicator in combination than does either one by itself. This indicates the strength of the hybrid detector for composition analysis.

It may be conceptually useful to think of the surface array as providing two measured quantities for each shower: ρ_{mu}, the muon density one km from the core, and ρ_{em}, the electromagnetic particle density 1 km from the core. Given any specific model (like Sibyllized Mocca, for example), there is a mapping from shower energy and primary mass (E,A) to (ρ_{mu}, ρ_{em}). The map gives the expected values for the measured quantities, determined by many simulations of showers with fixed E and A. (The mapping also depends on zenith angle, but it can be determined separately for every zenith angle.) Figure 5 shows this mapping schematically. The inverse mapping is also well defined, and this is how the measured quantities are used to infer E and A. For any measured pair

(ρ_{mu}, ρ_{em}), there is a unique energy and mass combination which gives that pair as the expected measured quantities. It is not required that the energy or mass be a simple function of the two measured quantities.

Energy and primary mass can be regarded as functions on the space of measured quantities. Curves of constant A, when mapped to (ρ_{mu}, ρ_{em}) space, tend to be diagonal lines in (ρ_{mu}, ρ_{em}) space. (Increasing E while keeping A fixed tends to increase both ρ_{mu} and ρ_{em}.) The curves of constant E are diagonals transverse to the constant-A curves. (Increasing A while E is fixed tends to increase the muon content but decrease the electromagnetic particles since ground level would be further past the maximum of the more rapidly developed shower.)

Mapping all recorded showers to (E,A) space yields a 2-dimensional histogram. Fixing an interval of A-values then gives the energy distribution for that mass component; fixing an energy range gives the mass distribution at that energy.

Similarly, you can think of the fluorescence detector as providing two measured quantities: E_{em}, the electromagnetic cascade energy, and X_{max}, the atmospheric depth of the cascade maximum. There is also a two-way mapping between this space and the (E,A) space. In this case, the curves of constant E are roughly parallel to the lines of constant E_{em}. The constant-A curves slope upward in X_{max} with increasing E in accordance with the elongation rate. It should be noted that the Fly's eye data, in this picture, originally gave a 2-dimensional scatter plot which was unphysical inasmuch as it extended to A-values in excess of 56. This suggested that the hadronic interaction model used to map from (E_{em},X_{max}) to (E,A) was unsatisfactory. The Gaisser-Stanev-Tilav minijet model (similar to Sibyll) was adopted to bring the scatter plot into the physically sensible region [11]. It has been argued [12] that any plausible model which is physically acceptable in this sense will preserve the observed feature of the scatter plot points moving to lower A-values with increasing energy. Hence the Fly's Eye data have been used both to constrain the hadronic interaction models and make a statement about composition changing over the measured energy range.

The picture of figure 5 provides a useful way to exhibit the advantage of a hybrid detector. A shower measured in hybrid mode gives a rectangular error box in both (ρ_{mu}, ρ_{em}) space and (E_{em},X_{max}) space. Their images in (E,A) space should overlap, and the true energy E and mass A should be in the intersection region. If the error box images from the two methods are systematically incommensurate, then there is a clear indication of systematic measurement errors or, perhaps more likely, an inappropriate model for the mappings. Once the defects are corrected, the dual measurements will give invaluable cross checks, shower by shower. Together, they should restrict the allowed range of A for each shower more than either component could by itself.

The picture of figure 5 also clarifies what it means to "train the surface array for energy determination." The fluorescence detector's E_{em} provides a reliable estimate for E. The hybrid data set is used to make sure that the mapping from (ρ_{mu}, ρ_{em}) space to (E,A) at least gets the energy right. The surface array by itself can then be trusted to determine the energy spectrum with the full data set. Even if the energy resolution is not as good as for the hybrid data set, at least the systematic errors should be eliminated. In a similar way, the hybrid data set may be able to validate (or adjust) the composition determination that is based on the larger data set of shower measurements by the surface array alone.

The analysis here has focused on just two measurable quantities for the surface array and the fluorescence detector. The analysis might also be able to take advantage of the signal rise time and a lateral distribution steepness parameter in the case of the surface array. With the fluorescence detector, one can try to measure also the longitudinal profile width (e.g. full width half maximum in g/cm^2) and the steepness of the profile's rising edge. These extra parameters may provide additional sensitivity to the primary mass when used in a multi-dimensional analysis.

Much careful work has been done in analyzing the capability of the Auger surface array on its own to measure shower energies and primary masses. Results can be found in the Design Report and Auger technical notes [13].

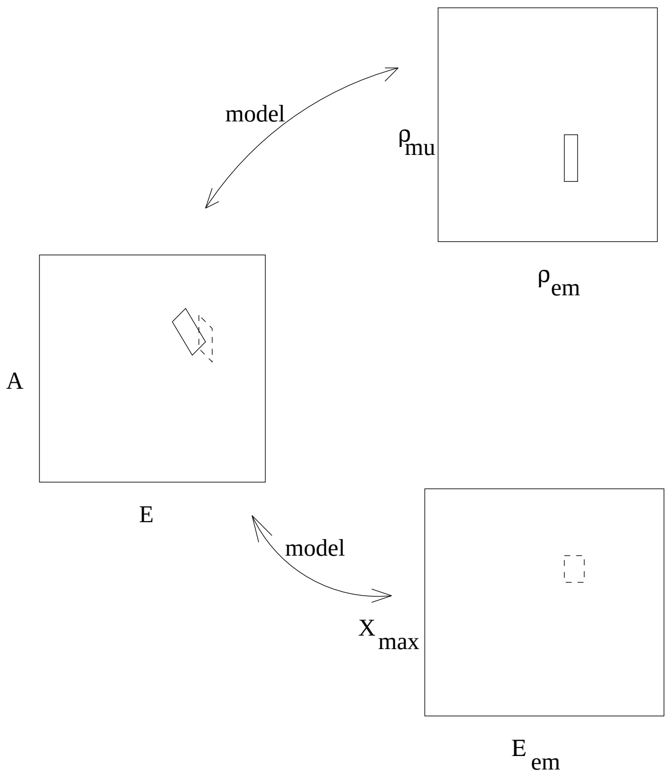

Figure 5: Shower simulations with a specific hadronic model give mappings from energy and mass (E,A) both to surface array quantities (ρ_{em}, ρ_{mu}) and to fluorescence detector quantities (E$_{em}$,X$_{max}$). A measured shower gives an error box in each space of measured quantities, and these can be mapped back to a pair of error boxes in (E,A) space.

4 The all-fluorescence alternative

It can be argued that a stereo fluorescence detector has better angular resolution and better energy resolution than a surface array. Even though the hybrid detector should have resolution equal to that of a stereo fluorescence detector, the vast majority of the Auger showers will be measured only by the surface array. Would it be more sensible to build a stereo fluorescence detector in each hemisphere and dispense with the surface array? This question was posed by the Fermilab Physics Advisory Committee, and it is sure to arise again during the review of the Auger proposal.

A variety of reasons can be cited for why the Auger design calls for a surface array with a fluorescence detector of matching aperture. Here are some:

1. The surface array has sensitivity to the shower muon content, and this is potentially the most powerful single handle on the primary mass.

2. Although the analysis of surface array data has more hadronic model dependence than analysis of fluorescence detector data, the measurements themselves are simpler. The techniques are well understood by a large community of high energy physicists. They have been used for extremely high energy cosmic ray observatories at Volcano Ranch, Sydney, Haverah Park, Yakutsk, and Akeno. The Fly's Eye is so far the only successful fluorescence detector observatory. Only a small number of physicists are familiar with the subtleties of the method, which go well beyond the tasks of understanding the detector's optics, photosensors, and electronics and the continual calibration of those detector components. Although the atmospheric fluorescence efficiency has been measured as a function of temperature and pressure at the relevant wavelengths [14], to make use of that information requires accurate modeling of the (variable) vertical structure of the atmosphere. In using the signal light flux to infer the shower size, it is necessary also to correct for light scattered to the detector from the strong Cherenkov beam and for attenuation of light between the shower and the detector. The attenuation is due to (variable) aerosol scattering as well as the predictable Rayleigh scattering. It is not obvious that the atmosphere can be monitored well enough to measure shower profiles precisely at great distances and to compute the exposure accurately enough for a reliable energy spectrum at the highest energies using an all-fluorescence observatory.

3. The hybrid detector has built-in cross checks on the methods of both techniques.

4. The hybrid detector has shower-by-shower cross checks on those shower measurements that will be used to determine the energy spectrum and composition.

5. The all-fluorescence option is more expensive. Approximately \$20M is budgeted for the Auger fluorescence detectors, apart from central computer stations, etc. The spacing has been chosen so that every 10 EeV shower landing in the array (on clear dark nights) will be observed at close enough range for a reliable measurement by a at least one eye. For an all-fluorescence detector to achieve a collecting power equal to that of the Auger surface array (i.e. compensate for the 10% duty factor due to clear moonless nighttime operation), 10 times as many fluorescence detectors would be needed. Each eye must also be upgraded so that it sees far enough that every shower will be seen by at least 2 eyes. (One of them can be somewhat farther away.) The upgrade might not be so very expensive, for example by increasing mirror sizes. Still, the total cost would be more than \$200M. This should be compared with the Auger surface array detector cost of \$50M

or the hybrid cost of \$70M, not counting the costs for central facilities and computer operations.

The all-fluorescence alternative can be made to look less expensive than this \$200M estimate in various ways:
(i) Raise the energy at which the 14,000 km^2·sr·yr/yr exposure rate pertains. In that case its cost should be compared with a simpler Auger configuration optimized for the same higher energy. (Bigger spacing between water tanks reduces the number of tanks required, and the Auger fluorescence detectors can also be simplified.)
(ii) Increase the spacing between fluorescence detectors, even if it means that many showers will not be observed from closer than 20 km. The Auger Collaboration has rejected the idea of profile measurements from such large distances because of concern about atmospheric variability and the impossibility of perfect monitoring.
(iii) Abandon the WBS cost estimate procedure and include only basic hardware costs. The cost should then be compared with a reduced Auger cost estimate based on the same method.

5 Summary

The Auger Observatory design is a hybrid detector consisting of a giant surface array together with a fluorescence detector of matching aperture. The reasons for employing both techniques include the following:

• A surface array is the cost-effective way to achieve the enormous collecting power which is especially important for the anisotropy analyses. The cost per shower, including the cost of the Auger fluorescence detectors, is less than 1/3 what it would be for an all-fluorescence detector that is designed to have a detector within 20 km of each shower.

• A continuously operating surface array is desirable for obtaining uniform exposure in right ascension and time-invariant declination acceptance.

• The fluorescence detector provides a model-independent measure of the electromagnetic shower energy. This is a calorimetric lower bound for the cosmic ray energy and can be scaled to obtain the best estimate for the total shower energy. The hybrid data set will yield an unambiguous energy spectrum.

• Measurements of both X_{max} and muon density for a shower of known energy give two handles on the primary mass which, together, are more powerful than either by itself. The hybrid data set will therefore provide a sensitive determination of the cosmic ray particle types.

• Hybrid shower measurements provide valuable cross checks between the surface array and fluorescence methods. There is a history of dispute and skepticism between advocates of the different methods. The hybrid detector offers the only sure way to resolve those differences and gain the confidence of the entire community. Moreover, without both components, it would be impossible to compare in detail the Auger results with those from all the other cosmic ray experiments.

• By comparing surface array measurements with fluorescence detector measurements shower-by-shower in hybrid mode, the analysis techniques for the surface array by itself can be tuned so that showers measured without the fluorescence detector can be used for a high-statistics determination of the energy spectrum and composition.

Acknowledgements. Thanks to Brian Fick, Jim Cronin, and Carlos Hojvat for commenting on the draft version of this note.

References

[1] J.W. Cronin, 1992 memo EFI 92-08

[2] D.J. Bird et al., *Phys. Rev. Lett.* **71**, 3401 (1993)

[3] N. Hayashida et al., *Phys. Rev. Lett.* **77**, 1000 (1996)

[4] T. Stanev et al., *Phys. Rev. Lett.* **75**, 3056 (1995)

[5] F.A. Aharonian & J.W. Cronin, *Phys. Rev.* **D50**, 1892 (1994)

[6] B.R. Dawson, "Hybrid simulations of a 3-eye system with dual mirrors," Auger technical note GAP-96-018 (1996)

[7] P. Sommers, "Large-scale ground array with monocular HiRes eye: shower geometry reconstruction," UMC Memo, UT920403, 1992

[8] P. Sommers, *Astroparticle Physics* **3**, 349 (1995)

[9] B.R. Dawson et al., *Astroparticle Physics* **5**, 239 (1996)

[10] B. Fick, "Hybrid array shower trajectory determination using the MIA and HiRes detectors," proceedings of the Utah workshop 1996 (to appear)

[11] T.K. Gaisser et al., *Phys. Rev.* **D47**, 1919 (1993)

[12] L.K. Ding et al., "Re-examination of cosmic ray composition around 10^{18} eV from Fly's Eye data," to appear in *Ap. J.* (1997)

[13] Auger technical notes (GAP papers) are available on the Web at URL http://tsswww.fnal.gov/Giant_Array_Project/GAP_Welcome.html

[14] T. Kakimoto et al., *Nucl. Inst. Meth.* **A372** 527 (1996)